Dual-band and polarization-insensitive terahertz absorber based on fractal Koch curves*

Ma Yan-Bing(马岩冰)[a)†], Zhang Huai-Wu(张怀武)[a)], Li Yuan-Xun(李元勋)[a)b)], Wang Yi-Cheng(王艺程)[a)], Lai Wei-En(赖伟恩)[a)], and Li Jie(李 颉)[a)]

[a)] State Key Laboratory of Electronic Films and Integrated Devices, University of Electronic Science and Technology of China, Chengdu 610054, China
[b)] Institute of Electronic and Information Engineering, University of Electronic Science and Technology of China, Dongguan 523808, China

(Received 9 July 2013; revised manuscript received 28 October 2013; published online 1 April 2014)

We report the design, fabrication, and characterization of a dual-band and polarization-insensitive metamaterial absorber (MA), which consists of periodically arranged fractal Koch curves acting as the top resonator array and a metallic ground plane separated by a dielectric spacer. Compared with conventional MAs, a more compact size and multi-frequency operation are achieved by using fractal geometry as the unit cell of the MA. Both the effective medium theory and the multi-reflection interference theory are employed to investigate the underlying physical mechanism of the proposed terahertz MA, and results indicate that the latter theory is not suitable for explaining the absorption mechanism in our investigated structure. Two absorption peaks are observed at 0.226 THz and 0.622 THz with absorptivities of 91.3% and 95.6% respectively and good agreements between the full-wave simulation and experimental results are achieved.

Keywords: metamaterial absorber, terahertz, fractal geometry

PACS: 81.05.Xj, 42.25.Bs, 42.60.Da **DOI:** 10.1088/1674-1056/23/5/058102

1. Introduction

Artificial metamaterials have attracted extraordinary attention owing to their unique features which generally are not available in nature. The realization of near-unity absorption is the most important functionality among many metamaterial applications. Since the first MA was proposed by Landy *et al.*,[1] many efforts have been focused on extending the applications of this kind of device to the terahertz (THz) regime by dimension scaling and manufacturing them by conventional micro-fabrication technologies. In addition, during the past few years, a great number of MAs with different structures such as electric-field-coupled (ELC) resonators,[2,3] cut-wire (CW),[1,4] and frequency selective surfaces (FSS),[5–7] have been reported. However, almost all of these pioneering MAs have only one resonance response, which limits their potential applications in spectroscopic detection and phase imaging of prohibited drugs and explosive materials that show distinct absorptions or "fingerprints" at multiple frequencies. Recent research progress showed that there are four approaches available to realize the multi-band MAs: the first way is to combine two or more resonators with different structures and resonant frequencies into a unit cell;[2,8,9] the second way is to form a super-unit-cell superposed by several sub-lattices,[10–12] each having the same structure but different size; the third way is to place identical resonant elements oriented in a rational arrangement;[13,14] the fourth way is to use multiple vertically stacked layers.[15] However, these approaches suffer from two issues: the former three have the problem of a large unit size and the last one has technical difficulties in manufacture.

In this paper, we present an alternative way to achieve multi-band operation by using fractal Koch curves as the top resonator array of the THz MA, which has two absorption peaks and the unit cells have a more compact size. Different from the four methods mentioned above, all the unit cells of the fractal MA are arranged in the same layer with the same geometry, size, and orientation. The dual-band operation is originated from the self-similar current distribution on the fractal surface[16,17] rather than from the combination of different resonant geometries, different sizes or different orientation and arrangement.

This paper is organized as follows. In Section 2, we start with the two analysis methods: effective medium theory and multi-reflection theory. Then advantages of the fractal absorber over conventional rectangle-shaped MA are demonstrated. The fabrication and measurement of a prototype for validating the numerically predicted performance are presented in Section 3, where good agreements between simulation and measurement results are achieved.

2. Design and characteristics

2.1. Theoretical interpretation

The schematic design of the fractal MA is shown in Fig. 1, which consists of a top resonator array of the second-order

*Project supported by the National Natural Science Foundation of China (Grant Nos. 60721001, 51132003, and 61171047), the National Natural Youth Fund of China (Grant No. 61001025), and the National Programs for Science and Technology Development of Guangdong Province, China (Grant No. 2010B090400314).

†Corresponding author. E-mail: mayanbing_uestc@163.com

© 2014 Chinese Physical Society and IOP Publishing Ltd

Koch curves repeated in the x and y directions, and a ground plane separated by a polyimide dielectric spacer with thickness $d = 22$ μm and relative permittivity $\varepsilon_r = 2.9(1 - 0.02j)$. The periodicity is $p = 300$ μm, and the length and width of the Koch curve are $L = 190$ μm and $w = 7.5$ μm, respectively. Finite-element numerical simulation is carried out by using the CST Microwave Studio, in which a lossy metal Cu with conductivity $\delta = 5.8 \times 10^7$ S/m is used to model the Koch curves and the metal ground. Periodic boundary conditions are applied to the side walls parallel to the z direction. The ports are added at the front and back surfaces of the unit cell for the electromagnetic wave incidence and transmission. The absorption is calculated as $A(w) = 1 - R(w) - T(w)$, where $R(w)$ and $T(w)$ represent the reflectivity and transmission as functions of angular frequency w, respectively. The simulated reflection and absorption are demonstrated in Fig. 2, showing that the absorption spectra reach the maximum of 99.2% and 99.97% at frequencies 0.23 THz and 0.64 THz, respectively.

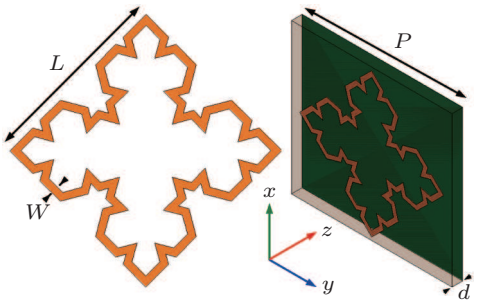


Fig. 1. (color online) Perspective of the unit cell based on the fractal pattern of the second-order Koch curves.

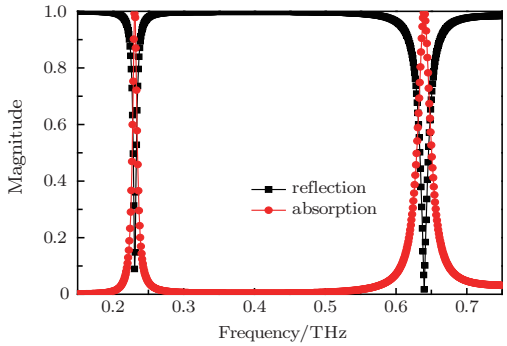


Fig. 2. (color online) Reflection and absorption of the fractal MA under normal incidence.

Almost all the pioneering work on MAs followed the theory of bulk effective medium, where the MA is considered as an effective medium characterized by electric permittivity $\varepsilon(w)$ and magnetic permeability $\mu(w)$. The permittivity is attributed to the electric resonance of the top resonator array, and the permeability is due to the magnetic resonance resulting from anti-parallel surface currents between the top metamaterial elements and the ground plane. Then the fundamental idea of designing an MA is to simultaneously tailor electric and magnetic responses to achieve suitable permittivity and permeability that will cause perfect impedance matching to free space at a specific frequency, i.e., $Z = \sqrt{\mu(w)/\varepsilon(w)} = Z_0$. Both real and imaginary parts of the wave impedance are shown in Fig. 3. At the two absorption peaks, the real relative impedance is nearly unity and the imaginary part is minimized, which means that impedance matching to the free space has been achieved at the air/absorber interface.

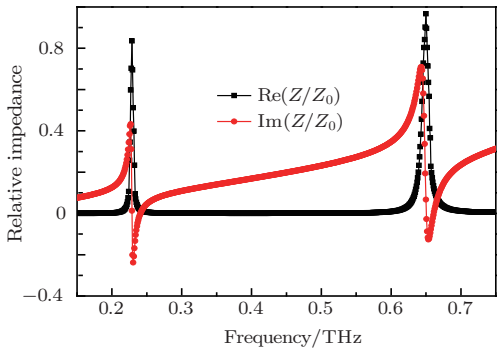


Fig. 3. (color online) Real part and imaginary part of the relative impedance.

To better understand the physical mechanism of the dual-band MA, the surface current analysis on the top resonator array and the bottom metallic ground can be used to gain insight into the two resonant modes. As shown in Fig. 4, the arrow indicates the direction of current flow and the currents are flowing in the opposite direction between the two metallic layers. Referring to the figure, it can be seen that two distinct resonant modes are evidently obtained.

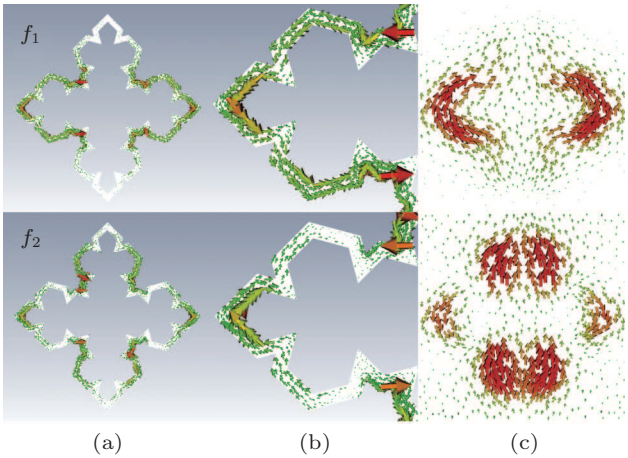


Fig. 4. (color online) (a) Current distribution for the two absorption peaks on the surface of the fractal Koch curve with the electric field E parallel to the x axis. (b) Partial enlarged details. (c) Current distribution on the ground.

The other alternative interpretation based on interference theory has been developed since it was introduced by Chen *et al.*,[18] in which the top resonator array and the ground are treated as zero-thickness impedance-tuned surfaces and the

metal-dielectric-metal structure forms a cavity where multi-reflection occurs. As illustrated in Fig. 5(a), at the air-spacer interface with the Koch curve array acting as some kind of metasurface, part of the incident THz radiation is reflected back to air with reflection coefficient $\tilde{r}_{12} = r_{12}\,\mathrm{e}^{\mathrm{j}\phi_{12}}$. The other part transmits into the spacer with transmission coefficient, $\tilde{t}_{12} = t_{12}\,\mathrm{e}^{\mathrm{j}\theta_{12}}$, and continues to propagate in the spacer until it reaches the ground plane and is reflected with reflection coefficient $\tilde{r}_{23} = \mathrm{e}^{\mathrm{j}\pi}$ towards the spacer/air interface where partial reflection/transmission occurs again with coefficients $\tilde{r}_{21} = r_{21}\,\mathrm{e}^{\mathrm{j}\phi_{21}}$ and $\tilde{t}_{21} = t_{21}\,\mathrm{e}^{\mathrm{j}\theta_{21}}$, respectively. These coefficients can be obtained by numerically simulated S-parameters of MA with moving ground plane (decoupled model).[5] The complex amplitude of all reflected waves from the air/spacer interface are superposed as[19]

$$R = \tilde{r}_{12} - \frac{\tilde{t}_{12}\tilde{t}_{21}\,\mathrm{e}^{\mathrm{j}2\tilde{\beta}}}{1+\tilde{r}_{21}\,\mathrm{e}^{\mathrm{j}2\tilde{\beta}}}, \tag{1}$$

where $\tilde{\beta} = k_0\sqrt{\varepsilon}d$ and k_0 is the free space wave number.

However, the interference theory is only suitable for explaining the absorption mechanism of weak coupling structures.[20,21] For certain geometries and dimensions of the resonators such as double-fishnet[22] and donut,[23] the interference theory is no more applicable owing to the strong coupling effect between the resonator array and the ground plane. To verify the interference theory for our structure, the metallic ground is removed to exclude the magnetic resonance.[5,24] The simulated transmission and reflection of the decoupled absorber (without ground) are depicted in Figs. 5(b) and 5(c). However, the calculated result derived from Eq. (1) has a large deviation from the full-wave simulated result as shown in Fig. 5(d), indicating the magnetic response originating from the near-field coupling between the resonator array and the ground plane can be significant and cannot be excluded completely from the two metallic layers. Thus, the multiple-reflection theory is not very suitable to explain the absorption mechanism of our investigated structure.

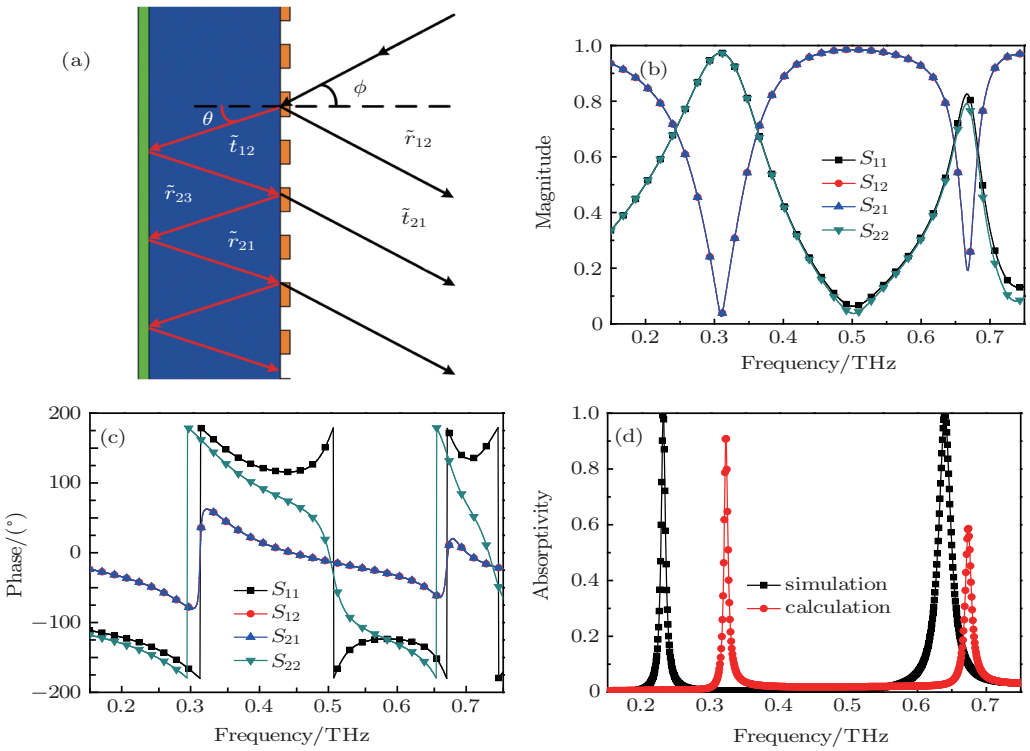


Fig. 5. (color online) (a) Multiple reflections and interference model of the MA, where the fractal resonator array is indicated by the dashed line at the air/spacer interface. (b) Amplitude and (c) phase of the transmission/reflection coefficients for the decoupled model. (d) Comparison between theoretically calculated and full-wave simulated absorptivity.

2.2. Benefits from fractal structure

Combining fractal geometry with electromagnetic theory has always been a promising research direction that has led to a plethora of new and innovative component designs by employing two important merits of fractals: space-filling and self-similarity. In a fractal structure, the boundary length diverges within a finite area as the fractal order increases to an infinite value. Therefore, it is possible to fabricate components with extremely small sizes as compared to the convention structure at the same operational frequency. In Fig. 6, the first absorption peaks are observed at 0.28 THz and 0.23 THz for the conventional MA and the second-order fractal MA, corresponding to $\lambda/2$ and $\lambda/2.6$, respectively, which occupy the same

dimension. Such red shift can be attributed to the increase in the line length with increasing fractal order. The resonance of the square ring originates from the dipole response.[25] The meandered side length of the Koch curve will lengthen the path of the surface current flowing through, which means such a device having a resonant structure will operate at a lower frequency. As a result, if operating at the same resonant frequency, the fractal structure will have a more compact size.

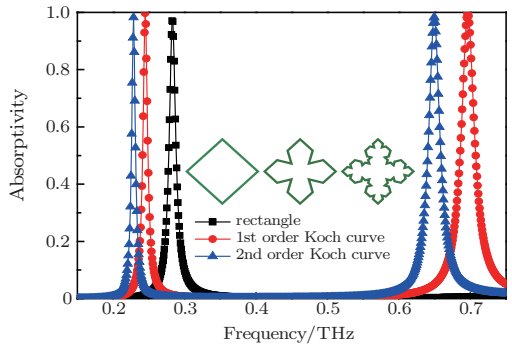


Fig. 6. (color online) Absorption spectra of the fractal MA in comparison with the conventional rectangle-shaped MA.

Multi-frequency operation can be very useful for spectroscopic detection because many explosives (C-4, HMX, RDX, and TNT) and illegal drugs (methamphetamine) have multiple characteristic absorption lines in the THz range. By tuning the metamaterial resonant responses at these specific absorption frequencies, the interaction between the terahertz wave and the materials will be dramatically enhanced. In addition, comparing measured THz spectra with known calibration spectra at multi-frequency points simultaneously can improve the measuring accuracy. On the other hand, multispectral and hyperspectral imaging can expand informativity of the inspected objects by detecting images simultaneously in multiple bands. Kuznetsov *et al.* reported a matrix structure of MAs for multispectral terahertz imaging[26] where each pixel was implemented by a single-band MA. Fractal structures have potential abilities to make metamaterials with multiple resonant properties which are not available for conventional structures. As shown in Fig. 6, two nearly perfect absorption peaks can be acquired by applying fractal Koch curves as the top resonator array, whereas only one absorption peak was achieved by using the conventional rectangle curve. Thus, if the single-band MA is substituted by the fractal MA, in the same area, the imaging system will have more pixels.

3. Fabrication and measurement

Due to the rotationally symmetric pattern of the square Koch curve around the z axis, the absorption response of the fractal MA is insensitive to the polarization of the incident wave. Figure 7 illustrates the simulated performance of the fractal MA with different polarizations of the incident wave. We can see that, with ϕ (the angle between the x axis and the electric field E direction) changing from 0° to 90°, the absorptivity almost remains unchanged, reflecting the insensitiveness of the fractal MA to the wave polarization.

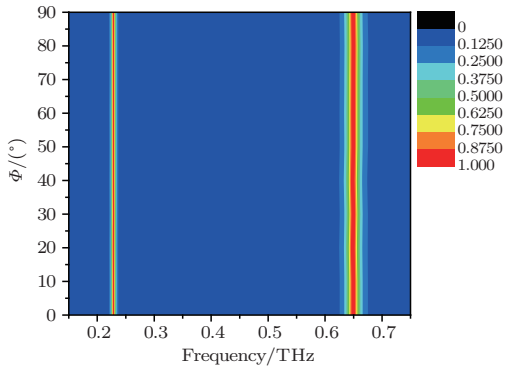


Fig. 7. (color online) Absorptivity as a function of polarization angle under the normal incidence.

In practical applications, electromagnetic wave is usually incident onto the absorber with an oblique angle, so the simulated absorptivity as a function of TE- and TM-polarized plane waves with the variation of incidence angle θ (the angle between the z axis and the incidence direction) are shown in Fig. 8. For the TE polarization, the parallel component of the H-field gradually diminishes as the incident angle increases. However, with TM polarization, the H-field remains unchanged at various incidence angles, which means the anti-parallel current between the two metallic layers (accountable to determine $\mu(w)$) can be efficiently driven for all

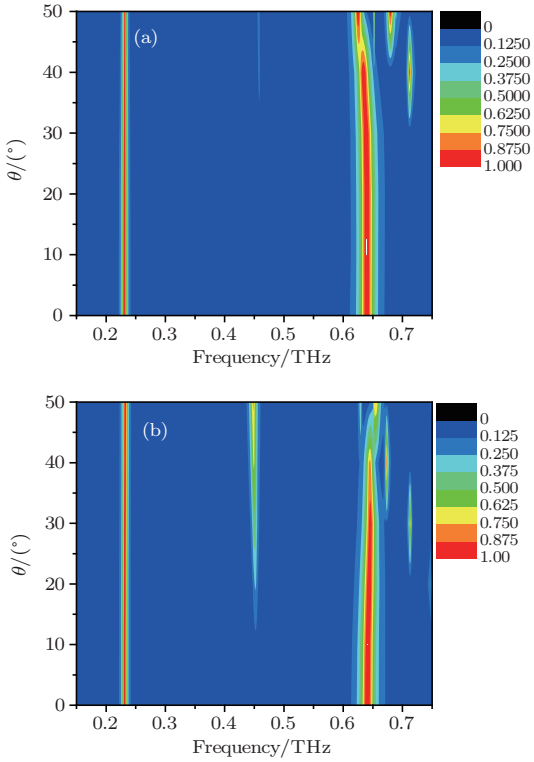


Fig. 8. (color online) Dependence of absorptivity on the incident angles under (a) TE and (b) TM polarization.

angles of incidence.[27] When the ground is removed, the magnetic resonance originated from the anti-parallel surface current between the two metallic layers will be no longer in existence and only the electric response of the resonator array remains under investigation. In Fig. 9, the resonance characteristics of the second-order Koch curve array at various incident angles are demonstrated. We can see that its second resonance response varies greatly with the incident angle, whereas the first resonance remains almost unchanged. This phenomenon can be ascribed to the intrinsic nature of the fractal Koch curve array, because its resonance characteristic is determined by its structure. Since these electric responses are primarily responsible for the determination of $\varepsilon(w)$, its variation with the incident angle will ruin the matched condition $Z = \sqrt{\mu(w)/\varepsilon(w)}$=$Z_0$ established under normal incidence.

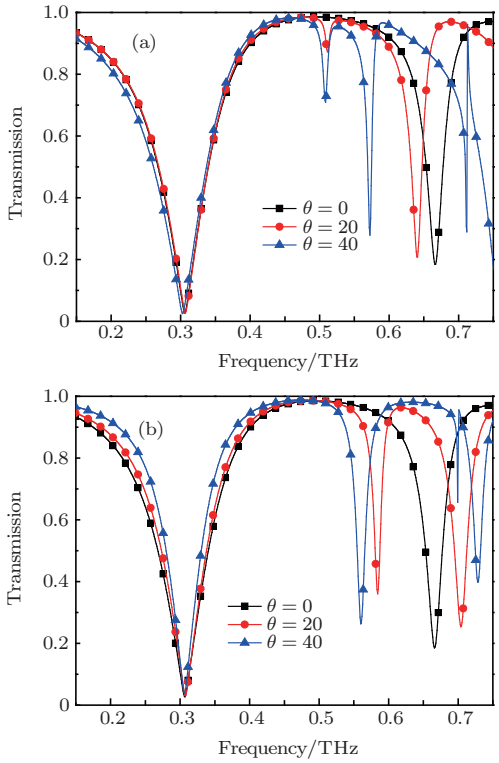


Fig. 9. (color online) Electric resonance response of the second-order Koch curve array for various incident angles under (a) TE and (b) TM polarization.

For the first absorption peak, because the first electric resonance response of the fractal Koch curve array almost remains unchanged at all incident angles, the performance of the fractal MA is mainly affected by the incident magnetic field. Under TE polarization, the first absorptivity gradually reduces as the incident angle increases. As shown in Fig. 8(a), the decreasing parallel component of the H-field has little effect on the first absorptivity, which still remains over 90% at 50°. Under TM polarization, the first absorptivity remains constant due to the invariant magnetic field. For the second absorption peak, the second electric resonance response of the fractal Koch curve array plays a dominant role because it varies greatly with increasing incident angle for both TE and TM polarization. As can be observed in Fig. 8, the second absorption efficiency and absorption frequency have undergone a considerable variation at the large incident angle.

The fractal MA shown in Fig. 10 is fabricated using conventional micro-fabrication techniques. A 200-nm-thick Cu ground plane is first deposited on a silicon substrate by radio-frequency magnetron sputtering, and then the polyimide spacer layer was spin-coated and thermally cured on the metal ground. 200-nm-thick fractal structures made of Cu were patterned on the spacer using the photolithographic method. The fabricated samples were measured under a THz time-domain spectrometer (TDS) in the reflection mode, with an incidence angle of about 30° off-normal and TE polarization due to the mechanical restriction. As shown in Fig. 11, the experimental results have two absorption peaks at 0.226 THz and 0.622 THz with absorptivities of 91.3% and 95.6% respectively, which agrees well with the simulated results.

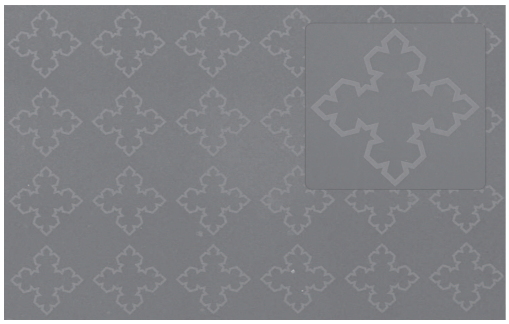


Fig. 10. Portion of the fabricated MA and the inset shows the enlarged unit cell.

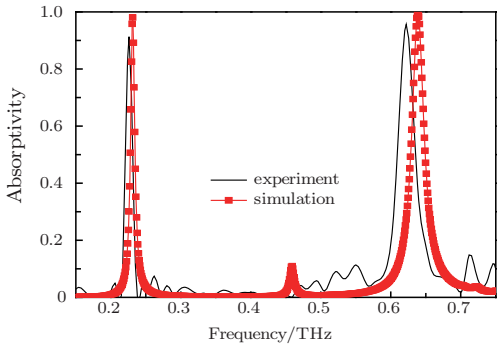


Fig. 11. (color online) Comparison of the absorption spectra between experimental and simulated results at an incidence angle of 30° under TE polarization.

4. Conclusions

In this work, we investigated both numerically and experimentally a dual-band polarization-insensitive THz MA, employing fractal Koch curves as the top resonator array. In virtue of the space-filling characteristics of fractal geometries, more compact unit size has been achieved as compared with the conventional MA. In addition, the dual-band operation

does not originate from the hybrid methods but from the self-similar current distribution on the fractal surface. From this point, we have provided an alternative new approach to realize the multi-frequency operation of the terahertz MA. The fractal MA we presented has been investigated by the two main theories: the effective medium theory and the multi-reflection interference theory, and we find that the latter theory is not very suitable for explaining the absorption mechanism. The fabricated fractal MA was measured by the THz-TDS system and good agreements between simulation and experimental results have been achieved.

References

[1] Landy N I, Sajuyigbe S, Mock J J, Smith D R and Padilla W J 2008 *Phys. Rev. Lett.* **100** 207402

[2] Tao H, Bingham C M, Pilon D, Fan K, Strikwerda A C, Shrekenhamer D, Padilla W J, Zhang X and Averitt R D 2010 *J. Phys. D: Appl. Phys.* **43** 225102

[3] Yuan Y, Bingham C M, Tyler T, Palit S, Hand T H, Padilla W J, Jokerst N M and Cummer S A 2008 *Appl. Phys. Lett.* **93** 191110

[4] Tao H, Landy N I, Bingham C M, Zhang X, Averitt R D and Padilla W J 2008 *Opt. Express* **16** 7181

[5] Chen H T 2012 *Opt. Express* **20** 7165

[6] Sun L K, Cheng H F, Zhou Y J and Wang J 2012 *Opt. Express* **20** 4675

[7] Liu L G, Wu W W, Mo J J, Fu Y Q and Yuan N C 2013 *Chin. Phys. B* **22** 047802

[8] Wen Q Y, Zhang H W, Xie Y S, Yang Q H and Liu Y L 2009 *Appl. Phys. Lett.* **95** 241111

[9] Gu C, Qu S B, Pei Z B, Xu Z, Liu J and Gu W 2011 *Chin. Phys. B* **20** 017801

[10] Li H, Yuan L H, Zhou B, Shen X P, Cheng Q and Cui T J 2011 *J. Appl. Phys.* **110** 014909

[11] Kollatou T M, Dimitriadis A I, Assimonis S D, Kantartzis N V and Antonopoulos C S 2013 *Prog. Electromagn. Res.* **136** 579

[12] Du Q J, Liu J S, Wang K J, Yi X N and Yang H W 2011 *Chin. Phys. Lett.* **28** 014201

[13] Li M H, Yang H L, Hou X W, Tian Y and Hou D Y 2010 *Prog. Electromagn. Res.* **108** 37

[14] Huang X J, Yang H L, Yu S Q, Wang J X, Li M H and Ye Q W 2013 *J. Appl. Phys.* **113** 213516

[15] Huang L and Chen H S 2011 *Prog. Electromagn. Res.* **113** 103

[16] Miyamaru F, Saito Y, Takeda M W, Hou B, Liu L, Wen W and Sheng P 2008 *Phys. Rev. B* **77** 045124

[17] Miyamaru F, Saito Y, Takeda M W, Liu L, Hou B, Wen W and Sheng P 2009 *Appl. Phys. Lett.* **95** 221111

[18] Chen H T, Zhou J F, O'Hara J F, Chen F, Azad A K and Taylor A J 2010 *Phys. Rev. Lett.* **105** 073901

[19] Born M and Wolf E 1999 *Principles of Optics: Electromagnetic Theory of Propagation, Interference and Diffraction of Light* (CUP Archive)

[20] Zhou J F, Chen H T, Koschny T, Azad A K, Taylor A J, Soukoulis C M and O'Hara J F 2011 arXiv:1111.0343v1 [physics.optics]

[21] Huang L, Chowdhury D R, Ramani S, Reiten M T, Luo S N, Azad A K, Taylor A J and Chen H T 2012 *Appl. Phys. Lett.* **101** 101102

[22] Dolling G, Enkrich C, Wegener M, Soukoulis C M and Linden S 2006 *Science* **312** 892

[23] Park J W, Van T P, Rhee J Y, Kim K W, Jang W H, Choi E H, Chen L Y and Lee Y 2013 *Opt. Express* **21** 9691

[24] Shen X P, Yang Y, Zang Y, Gu J, Han J, Zhang W and Cui T J 2012 *Appl. Phys. Lett.* **101** 154102

[25] Shen X P, Cui T J, Zhao J M, Ma H F, Jiang W X and Li H 2011 *Opt. Express* **19** 9401

[26] Kuznetsov S A, Paulish A G, Gelfand A V, Lazorskiy P A and Fedorinin V N 2012 *Prog. Electromagn. Res.* **122** 93

[27] Tao H, Bingham C M, Strikwerda A C, Pilon D, Shrekenhamer D, Landy N I, Fan K, Zhang X, Padilla W J and Averitt R D 2008 *Phys. Rev. B* **78** 241103